Effects of Memory on the Complex Rock-Fluid Properties of a Reservoir Stress-Strain Model

M. Enamul Hossain [a]; S. Hossein Mousavizadegan [a]; M. Rafiqul Islam [a]

[a] Department of Civil Engineering, Dalhousie University, Halifax, NS, Canada

PLEASE SCROLL DOWN FOR ARTICLE

Effects of Memory on the Complex Rock-Fluid Properties of a Reservoir Stress-Strain Model

M. Enamul Hossain,[1] S. Hossein Mousavizadegan,[1] and M. Rafiqul Islam[1]

[1]Department of Civil Engineering, Dalhousie University, Halifax, NS, Canada

Abstract: The memory based stress-strain model developed earlier by Hossain et al. (2007) has been solved numerically in this study. The derived mathematical model introduces the effects of temperature, surface tension, and pressure variations and the influence of fluid memory on the stress-strain relationship. The variation of shear stress as a function of strain rate is obtained for fluid in a sample oil reservoir to identify the effects of fluid memory. The stress-strain formulation related with the memory is taken into account, and we obtain the variation of it with time and distance for different values of α. The dependency of the stress-strain relation on fluid memory is considered to identify its influence on time. As pressure is also a function of space, the memory effects on stress and strain are shown in space with the pressure gradient change. The computation indicates that the effect of memory causes nonlinearity, leading to chaotic behavior of the stress-strain relationship. This model can be used in reservoir simulation and rheological study, well test analysis, and surfactant and foam selection for enhanced oil recovery.

Keywords: fluid memory, fluid viscosity, Newtonian fluid, non-Newtonian fluid, rheology

INTRODUCTION

It is well known that the petroleum industry drives the energy sector, which in turn drives modern civilization. Enhanced oil recovery (EOR) is an important topic of petroleum engineering research. While significant research has been conducted in this area, focused on improving oil recovery with different techniques, theoretical prediction methods for recovery schemes—a matter of utmost importance with cost implications in the millions of dollars on

    Address correspondence to M. Rafiqul Islam, Department of Civil Engineering, Dalhousie University, D510-1360 Barrington Street, Halifax, NS, Canada, B3J-1Z1. E-mail: Rafiqul.Islam@dal.ca

wrong uses for a single oil field—still suffer from certain shortcomings in their mathematical modeling (Abou-Kassem et al., 2006). The shortcomings can be listed as: 1) insufficient description of solid/liquid interaction, particularly under thermal constraints; 2) linearization of rheological data; and 3) linearization of governing equations. Furthermore, based on an insight in the information age, it has become possible to include phenomena that are considered to be intangible and beyond the scope of computational mathematics (Islam, 2006). Hossain and Islam (2006) have recently looked further into fluid rheology and fluid memory. They have presented an extensive review of the literature on this memory issue. They critically reviewed almost all the existing models and showed their limitations. They also showed how the memory of a fluid and the media play a great role in the stress-strain relationship.

There are very limited studies in the literature that describe this phenomenon clearly. Several non-Newtonian fluids behave chaotically at the time of flow through porous media, especially in some geothermal areas. As time passes, this chaotic behavior results in some precipitation of fluid minerals in the pore space, thus squeezing the flow path in the reservoir. However, some fluids may react chemically with the medium, enlarging the pores. Some fluids carry solid particles that may obstruct some of the pores. Pore size may also be changed by the minerals precipitated by the fluid and, finally, by temperature variations induced by the flux. The chaotic behavior of several non-Newtonian fluids leads the complexity in reality which is due to rheological change for memory and temperature. Newtonian fluid flow equations have been considered the ideal models for making predictions. Even non-Newtonian models focus on what is immediately present and tangible in regard to fluid properties (Gatti and Vuk, 2006; Chen et al., 2005).

Hossain et al. (2007) developed a new stress-strain model with memory to focus on he intangible problems and dimension of time and other fluid and media properties that have not been fully considered in existing models of fluid flow. They established the model with memory by including the continuous time function and identified the effects of considering memory and other properties such as viscosity, surface tension, temperature, and pressure. The model correlate the fluid viscosity, memory, activation energy, compressibility of fluid, pore thickness, porosity, and permeability of media with stress to describe the behavior of a fluid in porous media. They solved a part of the model that is related to only fluid memory, for which they established the effects of memory on space and time. This paper presents numerical solutions of the complete formulation presented by Hossain et al. (2007). It addresses the problems that arise if memory is ignored and identifies the impact of considering memory on the stress-strain relationship. This idea can be used in the understanding of viscoelastic fluid flow behavior in the reservoir. The commercial implications for the petroleum industry in revolutionizing present recovery practices along the lines of this study are considerable and important.

MATHEMATICAL MODEL

The effects of all parameters are considered to obtain the model for crude oil behavior in the reservoir formation. The effects of surface tension, temperature, pressure, and fluid memory are taken into account. The effect of surface tension is considered through the application of a Marangoni number (M_a) that explains the role of surface tension. This model gives the surface tension gradients along a gas–oil interface that provokes strong convective activity, called the Marangoni effect.

   The effect of memory is explained with a dominant variable, the fractional order of differentiation (α), and a constant, ratio of the pseudopermeability of the medium with memory to fluid viscosity (η). The effect of temperature on viscosity is applied by using the Arrhenius model. This model expresses the variation of temperature with an exponential function. The pressure variation is applied using Darcy's law. This law is widely accepted for describing fluid flow in porous media.

   The mathematical explanation and the derivation of the stress-strain formulation are described in Hossein et al. (2007). They gave the stress-strain relationship as follows:

$$
\tau_T = (-1)^{0.5} \times \left(\frac{\partial \sigma}{\partial T} \frac{\Delta T}{\alpha_D M_a} \right) \times \left[\frac{\int_0^t (t - \xi)^{-\alpha} \left(\frac{\partial^2 p}{\partial \xi \partial x} \right) d\xi}{\Gamma(1 - \alpha)} \right]^{0.5}
$$

$$
\times \left(\frac{6 K \mu_0 \eta}{\frac{\partial p}{\partial x}} \right)^{0.5} \times e^{\left(\frac{E}{R T_T} \right)} \frac{d u_x}{d y} \tag{1}
$$

   It should be mentioned here that the first part of Eq. (1) is the effects of surface tension; the second part is the effects of fluid memory with time and the pressure gradient; the third part is the effects of pressure, viscosity, and pseudopermeability; the fourth part is the effects of temperature on stress-strain equation; and the fifth part is the velocity gradient in y-direction, which is called the rate of velocity change, that is, the rate of shear strain. The second part is in a form of convolution integral that shows the effect of the fluid memory during the flow process. This integral has two variable functions of $(t - \xi)^{-\alpha}$ and $\partial^2 p / \partial \xi \partial x$, where the first one is a continuous changing function and second one is a fixed function. This means that $(t - \xi)^{-\alpha}$ is an overlapping function on the other function, $\partial^2 p / \partial \xi \partial x$, in the mathematical point of view. These two functions depend on the space, time, pressure, and a dummy variable.

CASE STUDY

The results of the stress-strain rate based on the model presented in Eq. (1) can be obtained by solving this equation. In this article, we focus on solving this formulation for stress-strain behavior in a real reservoir case. A reservoir of length (L = 5000.0 m), width (W = 50.0 m) and height, (H = 50.0 m) has been considered. The porosity and permeability of the reservoir are 30% and 30 mD, respectively. The reservoir is completely sealed and produces at a constant rate where the initial pressure is p_i = 27579028 pa (4000 psia). The fluid is assumed to be API 28.8 gravity crude oil with properties c = 1.2473×10^{-9} 1/pa, μ_0 = 87.4×10^{-3} Pa-s at 298 K. The initial production rate is q_i = 8.4×10^{-9} m^3/s, and the initial fluid velocity in the formation is u_i = $1.217 \times 10^{-5} m/s$. The fractional order of differentiation, α = $0.2 - 0.8$, Δx = 1000 m; Δt = $7.2 \times 10^4 s$ and t = 100 months, has also considered. The computations are carried out for Time = 20, 40, 60, and 80 months and at a distance of x = 1000, 2,000, 3,000, 4,000, and 4,500 meters from the wellbore. The pore size, h_f = 10 μm, ratio of the pseudopermeability of the medium with memory to fluid viscosity, η = 0.343249 and K = 0.25 are considered. To establish the Marangoni and temperature effects, ΔT = $(298.5 - 298.0)$ = $0.5K$; α_D = $6.75 \times 10^{-7} m^2/s$; M_a = 3.98; $\partial\sigma/\partial T$ = 0.165293 N/m-K; E = 50.52 KJ/mol; T_T = $298.5K$; R = 0.008314 kJ/mol-K have been considered. In solving this stress-strain model with memory, the trapezoidal method is used. All computation is carried out by Matlab 6.5.

To solve Eq. (1), it is necessary to obtain the pressure distribution along the reservoir. The pressure distribution is assumed to be modeled through the diffusivity equation in porous media. This equation has been derived by combining the continuity equation with Darcy's law as the momentum balance equation. This has been illustrated by Hossain et al. (2007), where they solved only the second part of the formulation, which is related to the effect of fluid memory and finding a numerical description for the same sample reservoir.

To study the fluid memory effects with the stress-strain model presented by Hossain et al. (2007), it is necessary to investigate Newton's viscosity model. The shortcomings and difficulties of this model for use in any reservoir modeling and simulation are pointed out in (Hossain el al., 2007). However, to investigate and study the stress-strain behavior, Newton's law of viscosity is treated as the benchmark because Newton's model has been considered the ideal model in fluid dynamics. Figure 1 shows the shear stress versus strain rate distribution based on this model. It illustrates that the stress is a linearly increasing function of the strain rate because this model does not take into account the majority of fluid and rock properties that practically exist in nature. The stress values calculated by this model are very small, which is unrealistic from a practical point of view and from the real stress data practically developed in a reservoir.
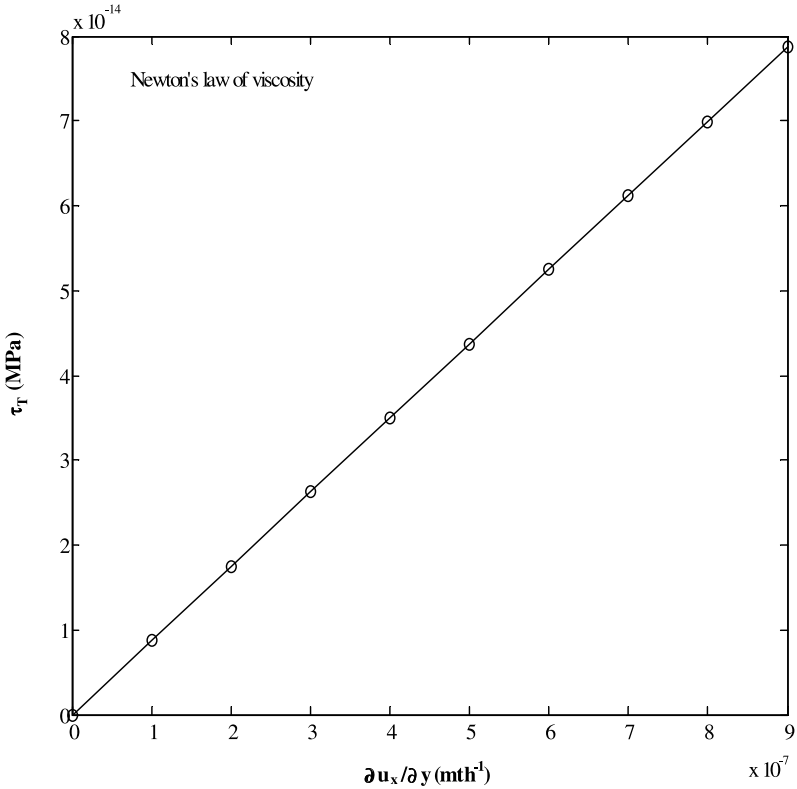
Figure 1. Shear stress (τ_T) variation with strain rate $\partial u_x / \partial y$ according to Newton's law of viscosity.

RESULTS AND DISCUSSION

Shear Stress Distribution based on Proposed Model

In nature, several non-Newtonian fluids behave chaotically at the time of flow through porous media, especially in some geothermal areas. As time passes, this chaotic behavior results in some precipitation of fluid minerals in the pore space, thus squeezing the flow path in the reservoir. However, some fluids may react chemically with the medium, enlarging the pores. Some fluids carry solid particles that may obstruct certain pores. Pore size may also be changed by the minerals precipitated by the fluid and, finally, by temperature variations induced by the flux. Lyford et al. (1998) pointed out that pore size may vary from 4.5 μm to 22.5 μm. Therefore, the chaotic behavior of several non-Newtonian fluids leads to complexity in reality, which is due to rheological change for memory and temperature. As a result, in the computation of proposed model, permeability

is varied from 20 mD to 50 mD. The fractional order of differentiation (α), which is related with memory, is taken in the range of $0.2 \leq \alpha \leq 0.8$ due to the computational accuracy and saving of computation time. The conventional computer takes a lot of time for one run. In solving the proposed model, pressure distribution is based on Darcy's diffusivity model. If we use the fluid memory concept to develop a diffusivity equation, it becomes a nonlinear integral partial differential second-degree equation. This makes the solution procedure more complicated. In this paper, this approach is ignored to simplify the solution. A spline curve fit is used in numerical simulation.

Dependence on Distance from the Wellbore

For numerical computation in solving the proposed model, the reservoir life is considered to be 100 months, and the distance from the wellbore to the outer boundary is considered to be $x = 1,000, 2,000, 3,000, 4,000,$ and $4,500$ m. Figures 2 to 6 show the shear stress variation as a function of strain rate at distances of 1,000, 2,000, 3,000, 4,000 and 4,500 m from the wellbore of the reservoir, respectively, for different α values. The stress increases nonlinearly with the increase of strain rate. Figure 2 shows the stress is in the range of 1.596×10^{-4} MPa to 4.923×10^{-4} MPa, whereas strain is 6.0×10^{-4} month^{-1} to 15.0×10^{-4} month^{-1}. For $\alpha = 0.2$, the range of stress is 1.596×10^{-4} MPa to 3.771×10^{-4} MPa. For $\alpha = 0.4$, the range of stress is 0.488×10^{-4} MPa to 0.765×10^{-4} MPa. This shows that with increase of α, the range tends to reduce as strain rate increases. Hossain et al. (2007) showed that this decrease continues up to $\alpha = 0.5$. Here, the stress range tends to increase at a range of 1.374×10^{-4} MPa to 1.783×10^{-4} MPa and 3.797×10^{-4} MPa to 4.923×10^{-4} MPa for $\alpha = 0.6$ and 0.8 respectively. It is clear in the figure that stress-strain is significantly affected by memory. In computation, it is identified that the integral part of the model with memory is more dominant than that of the gamma function with memory in the model. The integral part is in the range of 10 to 15 times greater when the gamma function is not considered (Hossain et al., 2007). In the permeability range of 20 to 50 mD the shear stress-strain has smooth nonlinear effects, which is more dominant when α increases.

Figure 3 displays the stress-strain plotting at a distance of 2,000 m from the wellbore. The figure shows that the stress-strain trend is similar to the one mentioned in Figure 2. However, the range of stress is reduced to an interval of 0.957×10^{-4} MPa to 3.036×10^{-4} MPa. It is noted that stress development is reduced compared with the stress level induced at 1,000 m distance from the wellbore.

Figure 4 shows the stress versus strain rate at a distance of 3,000 m from the wellbore of the reservoir for different α values. The stress-strain trend is similar to the one developed in Figure 3 except for its stress-strain range
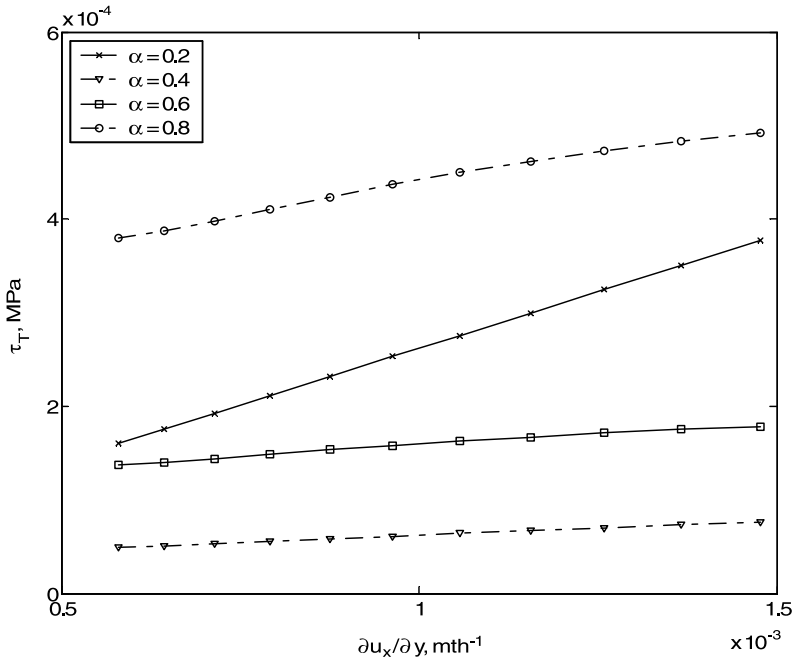
Figure 2. Shear stress (τ_T) variation as a function of strain rate $\partial u_x/\partial y$ for $x = 1,000$ m.
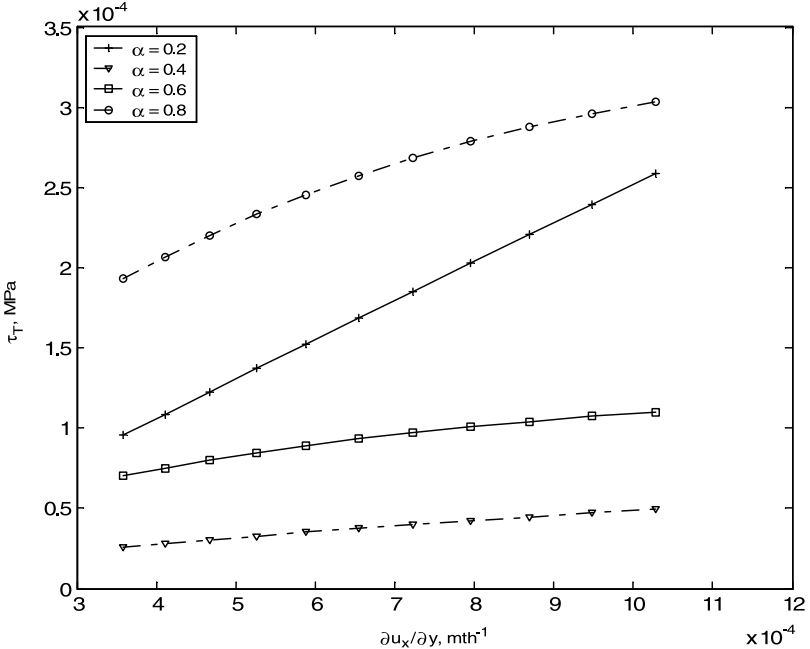
Figure 3. Shear stress (τ_T) variation as a function of strain rate $\partial u_x/\partial y$ for $x = 2,000$ m.
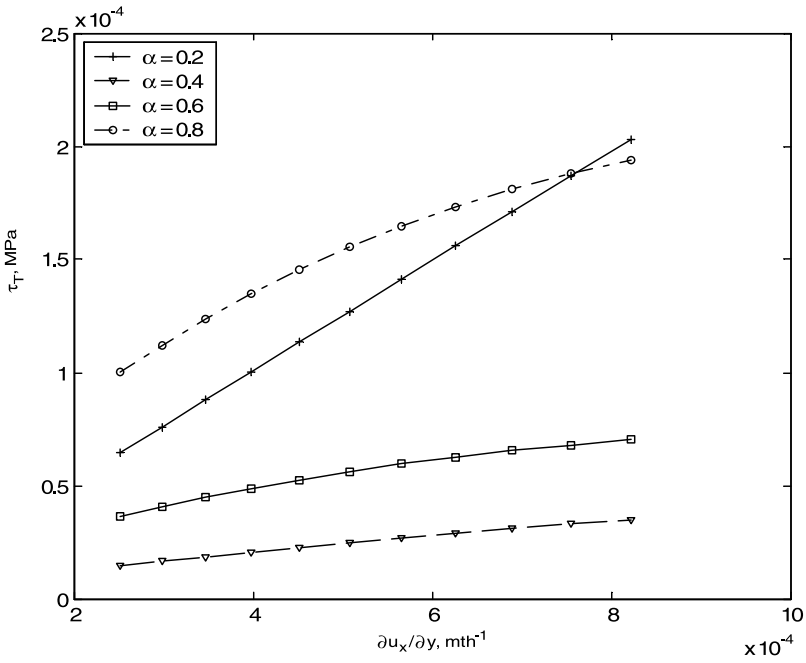
Figure 4. Stress (τ_T) and strain rate $\partial u_x / \partial y$ plotting for $x = 3{,}000$ m.
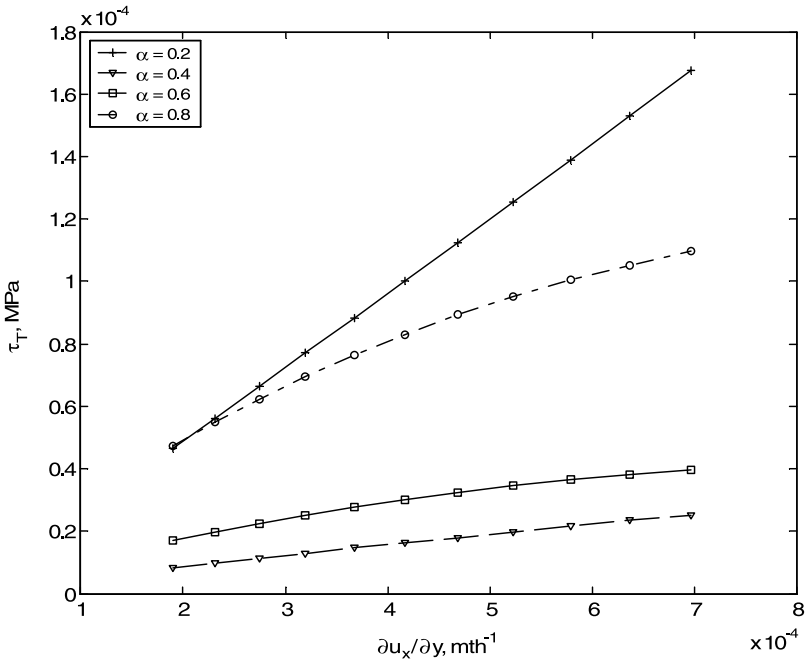
Figure 5. Stress (τ_T) and strain rate $\partial u_x / \partial y$ plotting for $x = 4{,}000$ m.
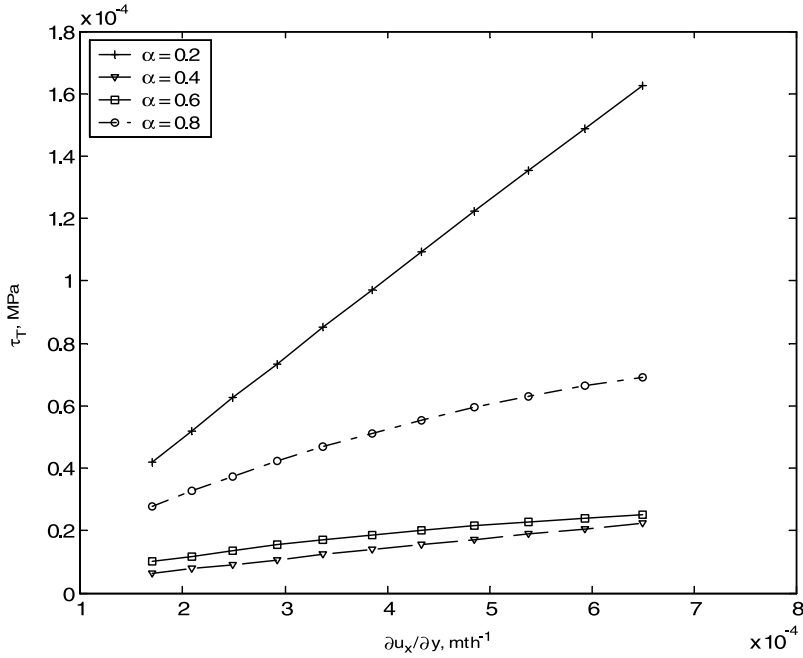
Figure 6. Stress (τ_T) and strain rate $\partial u_x / \partial y$ plotting for $x = 4,500$ m.

and a certain decrease of stress, as mentioned earlier. The range of stress is reduced, 0.645×10^{-4} MPa to 1.941×10^{-4} MPa.

Figure 5 shows the stress versus strain rate at a distance of 4,000 m from the wellbore of the reservoir for different α values. The stress-strain trend is similar to the one illustrated in Figure 4 except its stress-strain range. However, the range of stress is reduced, varying from 0.466×10^{-4} MPa to 1.096×10^{-4} MPa. It is noted that stress development is lower than that encountered at a 3,000 m distance from the wellbore.

Figure 6 shows the stress versus strain rate at a distance of 4,500 m from the wellbore of the reservoir for different α values. The stress-strain trend is similar to the one displayed in Figure 5 except its stress range is from 0.420×10^{-4} MPa to 0.692×10^{-4} MPa. Here the stress development is lower than the one encountered at a 4,500 m distance from the wellbore.

It is noted that stress development is greater around the wellbore. Figures 2 to 6 reveal that the shear stress is more sensitive to the memory factor around the wellbore than it is toward the outer boundary of the reservoir. Just after production, however in reality, there is stress relief around the wellbore due to pressure decrease, which exceeds the stress developed by the memory itself. Therefore, at the beginning of production, there is a drastic decrease of stress in Figures 2 and 3 for lower α values, and this level of stress development increases for higher α values. However, this decrease disappears

toward the outer boundary level, which is less affected in the initial stage of the production. After careful observation of the various figures dealing with stress-strain relationship dependence on distance from the wellbore, it can be concluded that the shear stress throughout the reservoir is sensitive to distance from the production wellbore. It decreases with the increase of distance from the wellbore. The same situation is encountered for the strain values, which decrease with distance from the wellbore as well.

Dependence On Reservoir Life from the Start of Production

For numerical computation in solving the proposed model, the distance from the wellbore toward the outer boundary is considered as $x = 3000\ m$ and the reservoir life is considered 20, 40, 60, and 80 months. Figures 7 to 10 show the stress-strain variation over the reservoir life of 20 to 80 months respectively for different α values.

Figure 7 shows the stress as a function of strain rate after 20 months from the date of production of the reservoir for different α values. The stress increases nonlinearly with the increase of strain rate. The stress is in the range of 2.2876×10^{-4} MPa to 6.9732×10^{-4} MPa for strain rate range of $0.69266 \times 10^{-3}\ months^{-1}$ to $1.3191 \times 10^{-3}\ months^{-1}$. With increase of
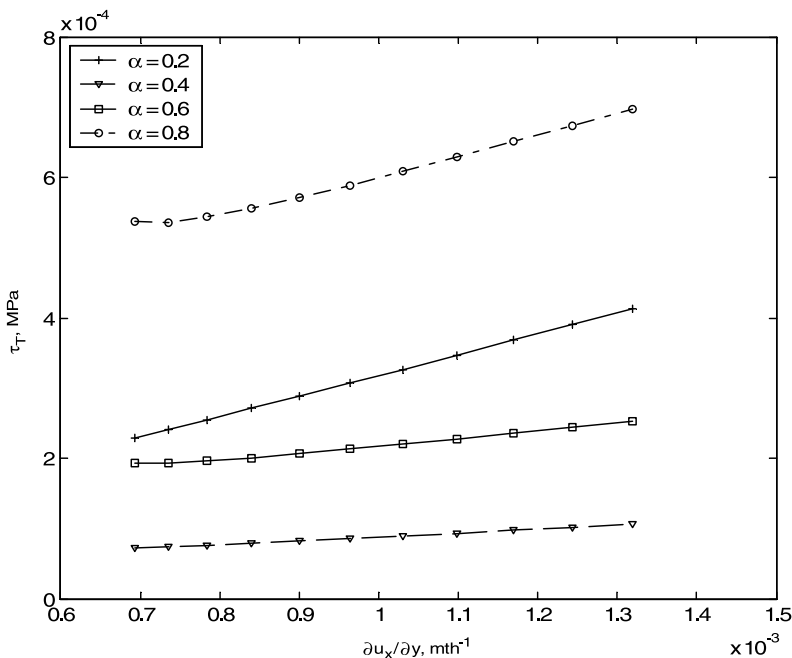
Figure 7. Stress (τ_T) and strain rate $\partial u_x / \partial y$ plotting for $x = 3,000$ m and time = 20 months.
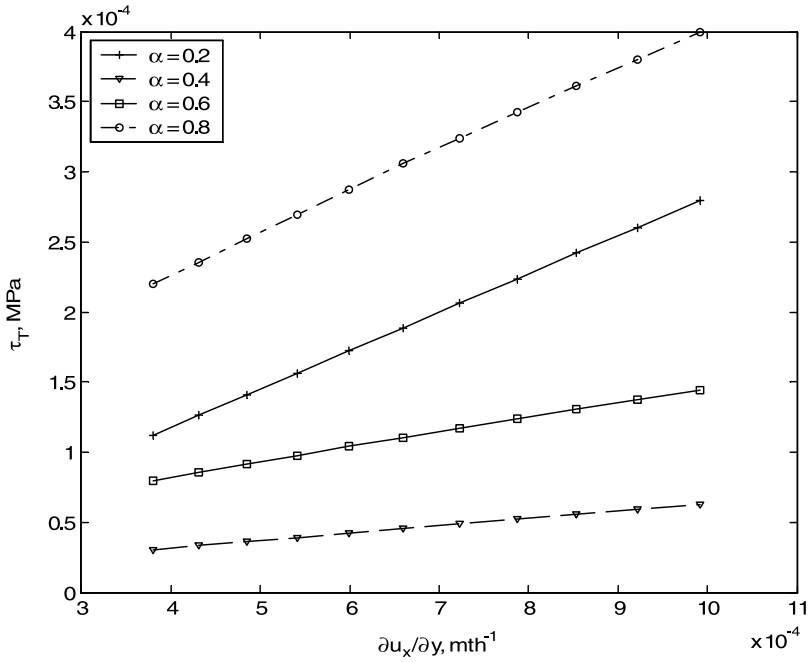
Figure 8. Stress (τ_T) and strain rate $\partial u_x / \partial y$ plotting for $x = 3{,}000$ m and time = 40 months.
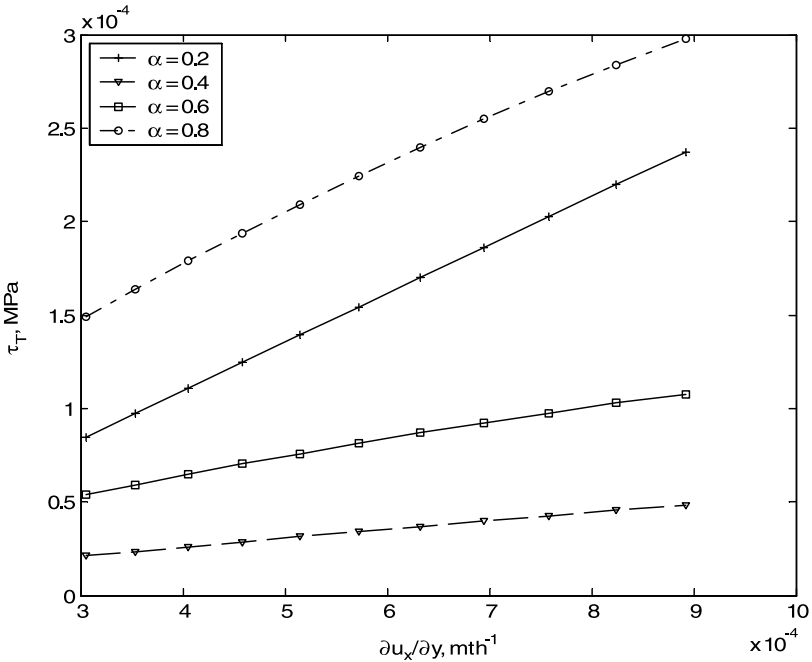
Figure 9. Stress (τ_T) and strain rate $\partial u_x / \partial y$ plotting for x = 3,000 m and time = 60 months.
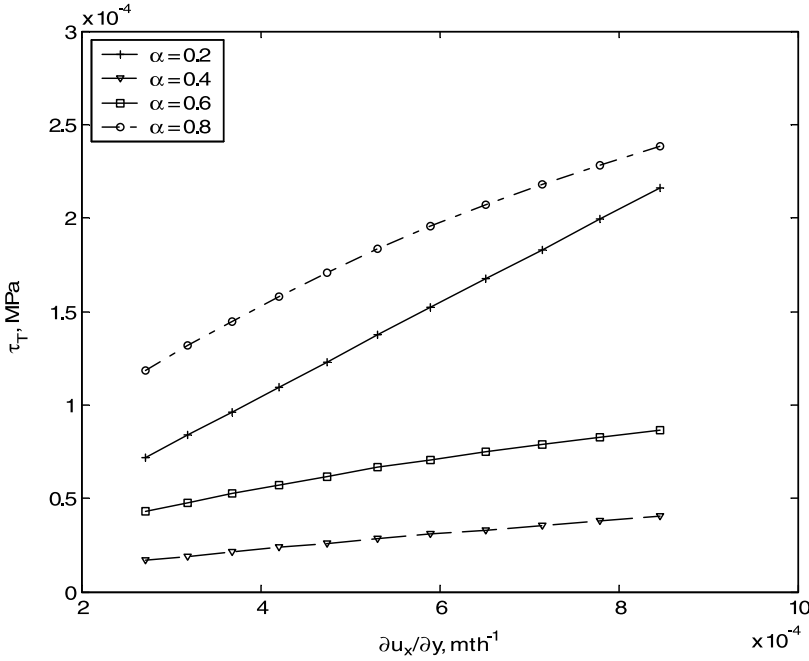
Figure 10. Stress (τ_T) and strain rate $\partial u_x/\partial y$ plotting for $x = 3,000$ m and time $=$ 80 months.

α from 0.2 to 0.4, the stress range tends to decrease as strain rate increases. However, with further increase of α (i.e., 0.6, 0.8), it tends to reduce the stress values with the increase of strain rate. This describes the chaotic behavior of fluid memory throughout the reservoir dimensions and life. It is clear in the figure that for $\alpha = 0.2$, stress increases faster with the slight increase of strain rate compared with higher α values. The figure also shows that stress increases with the increase of strain rate.

Figure 8 shows stress as a function of strain rate after 40 months from the date of production of the reservoir for different α values. The stress increases nonlinearly with the increase of strain rate. The stress is in the range of 3.0623×10^{-5} MPa to 3.9928×10^{-4} MPa for strain rate range of 3.8026×10^{-4} $months^{-1}$ to 9.9207×10^{-4} $months^{-1}$. However with increase of α, the stress range turns out to reduce as strain rate increases for $\alpha = 0.2$ to 0.4. After this α value, stress values turn out to increase with the same trend, which reveals the chaotic nature of the reservoir stress-strain behavior, as mentioned in Figure 7.

Figure 9 shows the stress versus strain rate after 60 months from the date of production of the reservoir for different α values. The stress increases nonlinearly with the increase of strain rate. The stress is in the range of 8.4405×10^{-5} MPa to 2.9777×10^{-4} MPa for strain rate range of $3.0487 \times$

10^{-4} $months^{-1}$ to 8.9239×10^{-4} $months^{-1}$. Both stress-strain values are lower than those of Figures 7 and 8, respectively. However, with increase of α, the range tends to reduce, as it does in the previous figures. It is clear in the figure that for $\alpha = 0.2$, stress increases faster with the slight increase of strain rate, compared with $\alpha = 0.4$ and 0.6.

Figure 10 shows the stress as a function of strain rate after 80 months from the date of production of the reservoir for different α values. The stress decreases nonlinearly with the increase of strain rate for different α values. This nonlinearity is more dominant when α increases. The stress is in the range of 7.1797×10^{-5} MPa to 2.3809×10^{-4} MPa for a strain rate range of 2.7068×10^{-4} $months^{-1}$ to 8.4646×10^{-4} $months^{-1}$. The trend of the curve and variation with α are similar to those of the previous Figures 7–9 except for the magnitudes of stress values.

In the short term, the stress values are at their highest levels due to the initial pressure buildup, as exhibited in Figures 7 and 8. These graphs considered in shorter reservoir life invoke the huge amount of stress due to the much higher pressure gradient compared with values corresponding to the longer life of the reservoir. However, the stress development starts to reduce when the reservoir life is increased, as shown in Figures 9 and 10. Then, in these cases, the reservoir stress-strain system is stabilized due to the long interval of time. Moreover, the nonlinearity is more visible when α increases. The overall study of the time effect on stress-strain dynamics shows that the shear stress throughout the reservoir is sensitive to reservoir life from the first production time. It decreases with the increase of time. The same situation is also encountered for the strain values, which decrease with time.

CONCLUSIONS

The comprehensive mathematical model introduced for stress-strain rate has taken into account the effect of variations of temperature, pressure, and surface tension and also the effect of fluid memory. The memory effect is introduced by a fluid flow model, for which the fractional order of differentiation and ratio of the pseudopermeability of the medium with memory to fluid viscosity exists.

The results show that the stress-strain rate relationship is influenced by a number of major parameters that have been considered during the development of the model. Among the parameters, fluid memory and fluid velocity have more impact on the stress-strain relationship. Moreover, the variation of distance and time defines a chaotic behavior with nonmonotonous trends of the stress-strain relationship, which is a strong indication of the memory effect.

This article reveals that the memory mechanism helps in interpreting the reservoir phenomenology in addition to other parameters such as matrix heterogeneity, anisotropy, and inelasticity. This model is more appealing

because the probable fluid properties and fluid media properties have been considered to develop this model, and its results match with existing available stress data.

ACKNOWLEDGEMENT

REFERENCES

Abou-Kassem, J. H., Farouq Ali, S. M., and Islam, M. R. (2006). *Petroleum reservoir simulation: A basic approach*. Houston: Gulf.

Chen, M., Rossen, W., and Yortsos, Y. C. (2005). The flow and displacement in porous media of fluids with yield stress. *Chem. Eng. Sci.* 60:4183–4202.

Gatti, S., and Vuk, E. (2006). Singular limit of equations for linear viscoelastic fluids with periodic boundary conditions. *Int. J. Nonlinear. Mech.* 41:518–526.

Hossain, M. E., and Islam, M. R. (2006). Fluid properties with memory: A critical review and some additions. Paper CIE 00778, *36th Int. Conf. Comp. Ind. Eng.*, Taipei, June 2–5.

Hossain, M. E., Mousavizadegan, S. H., Ketata, C., and Islam, M. R. (2007). A novel memory based stress-strain model for reservoir characterization. *Journal of Nature Science and Sustainable Technology* 1:653–678.

Islam, M. R. (2006). Computing for the information age. *36th Int. Conf. Comp. Ind. Eng.* Taipei, June 2–5.

Lyford, P., Pratt, H., Greiser, F., and Shallcross, D. (1998). The Marangoni effect and enhanced oil recovery part 1: Porous media studies. *Can. J. Chem. Eng.* 76:167–174.

NOMENCLATURE

A_{yz} cross sectional area of rock perpendicular to the flow of flowing fluid, m^2

c total compressibility of the system, $1/pa$

E activation energy for viscous flow, KJ/mol

h_f height in temperature gradient (height between the two points along the y-direction) or in other words, thin film thickness of flowing fluid, m

k	initial reservoir permeability, m^2
K	operational parameter
L	distance between production well and outer boundary along x direction, m
M_a	Marangoni number
p	pressure of the system, N/m^2
p_i	initial pressure of the system, N/m^2
q_x	fluid mass flow rate per unit area in x-direction, $kg/m^2 - s$
q_i	$Au = $ initial volume production rate, m^3/s
R	universal gas constant, $KJ/mole - K$
T	temperature, K
T	time, s
ξ	a dummy variable for time i.e., real part in the plane of the integral, s
u	filtration velocity in x direction, m/s
u_x	fluid velocity in porous media in the direction of x axis, m/s
y	distance from the boundary plan, m
ϕ	porosity of fluid media, m^3/m^3
σ	surface tension, N/m
α	fractional order of differentiation, dimensionless
α_D	thermal diffusivity, m^2/s
μ	fluid dynamic viscosity, $Pa\text{-}s$
μ_0	fluid dynamic viscosity at reference temperature T_0, $Pa\text{-}s$
μ_T	fluid dynamic viscosity at a temperature T, $Pa\text{-}s$
τ	shear stress, Pa
τ_T	shear stress at temperature T, Pa
$\dfrac{du_x}{dy}$	velocity gradient along y-direction, $1/s$
ΔT	$T_T - T_0 = $ temperature difference, K
ρ_0	density of the fluid at reference temperature T_0, kg/m^3
$p(x,t)$	fluid pressure, pa
η	ratio of the pseudopermeability of the medium with memory to fluid viscosity, $m^3 s^{1+\alpha}/kg$
$\left\lvert \dfrac{d\sigma}{dT} \right\rvert$	the derivative of surface tension σ with temperature; can be positive or negative, depending on the substance, $N/m\text{-}K$